

Universality of critical dynamics on a complex network

Mrinal Sarkar¹, Tilman Enss¹, and Nicolò Defenu²

¹*Institut für Theoretische Physik, Universität Heidelberg, 69120 Heidelberg, Germany and*

²*Institut für Theoretische Physik, ETH Zürich, Wolfgang-Pauli-Str.27, 8093 Zürich, Switzerland*

(Dated: March 21, 2024)

We investigate the role of the spectral dimension d_s in determining the universality of phase transitions on a complex network. Due to its structural heterogeneity, a complex network generally acts as a disordered system. Specifically, we study the synchronization and entrainment transitions in the nonequilibrium dynamics of the Kuramoto model and the phase transition of the equilibrium dynamics of the classical XY model, thereby covering a broad spectrum from nonlinear dynamics to statistical and condensed matter physics. Using linear theory, we obtain a general relationship between the dynamics occurring on the network and the underlying network properties. This yields the lower critical spectral dimension of the phase synchronization and entrainment transitions in the Kuramoto model as $d_s = 4$ and $d_s = 2$ respectively, whereas for the phase transition in the XY model it is $d_s = 2$. To test our theoretical hypotheses, we employ a network where any two nodes on the network are connected with a probability proportional to a power law of the distance between the nodes; this realizes any desired $d_s \in [1, \infty)$. Our detailed numerical study agrees well with the prediction of linear theory for the phase synchronization transition in the Kuramoto model. However, it shows a clear entrainment transition in the Kuramoto model and phase transition in the XY model at $d_s \gtrsim 3$, not $d_s = 2$ as predicted by linear theory. Our study indicates that network disorder in the region $2 \leq d_s \lesssim 3$ introduces strong finite-size fluctuations, which makes it extremely difficult to probe the existence of the ordered phase as predicted, affecting the dynamics profoundly.

I. INTRODUCTION

Phase transitions and critical phenomena are a much-studied research topic in statistical and condensed matter physics. By now, it is well known how large-scale geometry affects the universal behavior of phase transitions and critical phenomena. Most of the research, both in and out of equilibrium, focuses on regular Euclidean lattices. Renormalization group theory helps us understand this phenomenon for statistical systems on such a regular lattice. It predicts that the Euclidean dimension is the only relevant geometrical parameter in determining universality classes.

However, the situation is not so obvious when we have a system that breaks the translational invariance, such as disordered lattices, fractals, amorphous materials, or, in general, graphs or networks. Although a vast amount of literature has been dedicated to studying critical phenomena on disordered lattices in condensed matter and statistical physics, the same on a general graph or a complex network appears new to this list, drawing attention only recently. A complex network, formed by a set of nodes and links between them, also acts as a disordered system, where the disorder arises from structural heterogeneity: the degree distribution and its various moments [1, 2]. Based on the structural properties or inhomogeneity of the network, the critical dynamics on such a network may yield nontrivial and intriguing results.

Critical dynamics on complex networks finds many applications in diverse fields: epidemic spreading [3], brain dynamics [4], urban traffic on roads [5], and many others [6]. A pertinent question is: Which parameter determines the universality classes for critical systems on a general network? It is believed that the spectral dimen-

sion, more specifically, the “average spectral dimension” (d_s) of a network, is equivalent to the Euclidean dimension for lattices. The spectral dimension characterizes the scaling of the low-lying eigenvalues of the associated Laplacian of the network [7, 8]. If the first, smallest non-zero (Fiedler) eigenvalue vanishes in the thermodynamic limit, the network is said to have a finite spectral dimension [9, 10]. On the other hand, if it remains finite, the network is said to develop a spectral gap, implying infinite spectral dimension.

We ask a fundamental question: Given two networks with the same spectral dimension d_s , does the dynamics on both networks belong to the same universality class? Or, in other words, is the spectral dimension the only relevant parameter of a network that determines the universality class of the dynamics? This quest has been pursued in the field of statistical physics for a long time; however, a unique answer to it is still lacking. The relation between network geometry and dynamics is far from trivial. There are a few studies that generalize the analysis of lattices to networks. We must note that a complex network is fundamentally very different from a regular Euclidean lattice. For a network and a lattice with the same finite d_s , the eigenvectors of the network Laplacian may not be delocalized over the network like the Fourier basis on the Euclidean lattice. Instead, these eigenvectors may be localized on a few nodes, reflecting the symmetries present in the network. Also, this feature may depend on the properties of the network, thereby raising the fundamental question of the role of spectral dimension in determining the universality of the dynamics. Addressing this question is the key focus of our present work.

The nonlinearity in the dynamics and the heterogeneity in a complex network make, in general, such a study

analytically formidable [6]. Even numerically, one major problem lies in accessing networks of any spectral dimensions. To overcome this, we have employed a network where we can tune its spectral dimension continuously and thus have the freedom to work in any dimension $d_s \in [1, \infty)$ and test numerically various hypotheses or theoretical predictions [11].

To study the role of spectral dimension in determining the universality of the dynamics, we consider two fundamentally different kinds of dynamics on such a network: One is a nonequilibrium dynamics of a paradigmatic model of nonlinear dynamics, namely, the Kuramoto model showing spontaneous synchronization [12–15], and the other one is an equilibrium one, namely, the dynamics of a classical XY model, another paradigmatic model of statistical and condensed matter physics. First, we theoretically obtain the role of d_s on the phase and entrainment transition for the Kuramoto dynamics and test the theoretical predictions numerically. Next, we investigate the role of d_s for the universality of the phase transition of the classical XY model [16, 17]. One advantage of studying the Kuramoto model is that we can map it to the dynamics of the classical XY model in a certain limit: Making the natural frequencies of the oscillators identical, then going to a co-moving frame rotating at that identical frequency, and applying Gaussian white noise to the systems [18, 19]. This is equivalent to making the ‘quenched’ disorder of the natural frequencies an ‘annealed’ one (Gaussian white noise). In contrast to the usual nonequilibrium Kuramoto dynamics for quenched disorder, the dynamics in the case of annealed disorder (XY model) is now governed by equilibrium statistical mechanics. In this paper, we examine both cases in turn; more details will be provided in the subsequent section.

We show in this work for a given dynamics occurring on the network, under linear approximation, how the stationary-state fluctuations and phase correlations depend on the underlying network properties, namely, the density of eigenvalues of the network Laplacian and the stationary distribution of the coefficients (corresponding to the variables expressed in the eigenbasis of the Laplacian). In the context of the Kuramoto model and the classical XY model, we explicitly obtain these quantities, which further help us estimate the lower critical spectral dimension d_s of the associated phase transitions. Our main finding is that the linear theory predicts the lower critical dimension for entrainment and synchronization transition in the Kuramoto model as $d_s = 2$, and $d_s = 4$, respectively, and for the phase transition in the XY model it is $d_s = 2$. Our detailed numerical investigation agrees well with the theoretical prediction of synchronization transition in the Kuramoto model. However, it does not yield a clear signature of entrainment transition in the Kuramoto model and phase transition in the XY model in $2 \leq d_s \lesssim 3$. This indicates that the network heterogeneity in the form of bond disorder is harmless at dimension $d_s > 3$, whereas it plays a crucial role in the region $2 \leq d_s \lesssim 3$: It introduces strong

finite-size fluctuations, which vanishes very slowly in the thermodynamic limit. This, in turn, makes it extremely difficult to probe the existence of the ordered phase as predicted [20].

For a similar line of work, we cite Ref. [21] in the context of synchronization in the Kuramoto model at various spectral dimensions. Our theoretical results for the Kuramoto model match the prediction in Ref. [21], which validates our theory. However, our work is different from that in three contexts: First, we go beyond the Ref. [21] in that we have derived the expressions of the observables on a general ground, under the assumption that the dynamics (of interest) has a unique stationary state on the network, while it was obtained in the reference using an explicit solution of the deterministic Kuramoto dynamics. Second, our method is general in that it applies to both deterministic and stochastic dynamics on the network so long as it has a unique stationary state. Third, in Ref. [21], the numerical test was performed on a complex network manifold that generates discrete d -dimensional manifolds by gluing d -dimensional simplices along their $(d-1)$ -faces subsequently, whereas, in numerics, we tune spectral dimension in our model continuously. Another work in the similar line but for the second-order Kuramoto model on a lattice can be found in Ref. [22].

The paper is organized as follows. Sec II describes the graph/network we work on and defines our model of study along with the main queries addressed in this work. In Sec III, we derive our theoretical predictions for the stability of the ordered phase in terms of spectral dimension on a general network under linear approximation, thereby predicting the lower critical dimensions for the phase and entrainment transitions in the Kuramoto and XY models. Sec IV defines the observables to study numerically the associated transitions of the Kuramoto and XY dynamics. In Sec V, we provide our numerical results on phase and entrainment transitions of the Kuramoto dynamics, test our theoretical predictions, and discuss the possible role of graph disorder on the dynamics, while in Sec VI we study the same for the XY dynamics. The paper ends with conclusions in Sec. VII. Finally, Appendix A provides a derivation of the quantities required to compute fluctuations and correlation in the linear theory.

II. MODEL AND DYNAMICS

In this section, we first introduce the model, namely, the 1D Long-range random ring (1DLRRR or 1DLR3) network [11]. The network is constructed as follows: We first consider as a backbone a one-dimensional linear lattice of N sites with periodic boundary conditions, thus forming a ring. Next, any two sites i and j ($\neq i$) ($i, j = 0, 1, 2, \dots, N-1$) on the lattice are connected by a link with a probability $p_{ij} = 1/|i-j|^{1+\sigma}$, where $|i-j| = \min(|i-j|, N-|i-j|)$, and the parameter σ characterizes the scaling of the probability p_{ij} with distance.

The network does not contain any self-loops. The network is characterized by the adjacency matrix $A = \{a_{ij}\}$, with $a_{ij} = 1$ or 0 depending on whether the nodes i and j are connected or not, according to the link probability. Furthermore, we consider the network to be undirected and symmetric, i.e., $a_{ji} = a_{ij}$. The parameter σ controls the network properties: in particular, the degree distribution. By tuning the parameter σ , one could generate a sparse or dense network, or a network of tightly connected local networks with rare long-range links. For example, $\sigma = -1$ corresponds to a network with *all-to-all* connections, whereas $\sigma \rightarrow \infty$ corresponds to a 1D lattice with nearest neighbor connections only, and one can thus obtain a network with local and long-range links by tuning σ between these two extreme limits. We refer the reader to Ref. [11] for the basic network characteristics, e.g., the degree distribution and its mean, variance, etc., of this model.

In contrast to the well-studied 1D lattice model with long-range power-law decaying interactions [23], the present model is a network (1D lattice with additional long-range links) where the interaction strength is equal among all neighbors; however, the connection probability decays as a power-law. The coupling probability gives rise to randomness that violates the translational invariance and also acts as a source of quenched ‘bond-disorder’ in the system. This model has already been employed to investigate the critical properties of long-range epidemics [24] and percolation [25]. Also, critical dynamics of the XY model [26, 27], epidemic spreading [28] and self-avoiding walks [29] have been studied on a two-dimensional lattice version of it. A generalization of the present model is reminiscent of the Kleinberg model [30] of network science, showing the emergence of the small-world phenomenon [31], and was employed in the study of navigation problems [32–34].

The spectral properties of our 1DLR3 network are thoroughly investigated in Ref. [11]. By tuning the parameter σ continuously, this model allows one to realize the whole range of spectral dimension $d_s \in [1, \infty)$. This feature makes it a suitable candidate to investigate the universal behavior for critical models with both continuous and discrete symmetries.

To study the universality of the dynamics on such a network, we first work with the paradigmatic model of nonlinear dynamics, namely, the Kuramoto model, showing the spontaneous emergence of collective synchronization [12–15]. The model comprises a collection of L interacting limit-cycle oscillators residing at nodes of the network and of distributed natural frequencies. The phase $\theta_i(t) \in [0, 2\pi)$ of the i -th oscillator evolves in time as [12]

$$\frac{d\theta_i}{dt} = \omega_i + \frac{K}{\kappa_i} \sum_{j=1}^N a_{ij} \sin(\theta_j - \theta_i). \quad (1)$$

Here, $K \geq 0$ denotes the strength of coupling between the oscillators, $\omega_i \in (-\infty, \infty)$ is the natural frequency of the i -th oscillator, a_{ij} is the adjacency matrix for a

given network realization, and $\kappa_i = \sum_j a_{ij}$ is the degree of the i -th node. The scaling by κ_i of the second term on the right-hand side ensures that this term is well behaved in the limit $N \rightarrow \infty$ and, moreover, to screen out the effect of having heterogeneous degree distributions. The ω_j ’s are quenched-disordered random variables distributed according to a common distribution $G(\omega)$ with finite mean $\Omega_0 > 0$ and width $\Delta > 0$. By choice of a suitable frame of reference, the mean of the distribution Ω_0 can be set to zero without loss of generality. In our numerical simulations, the natural frequencies are drawn from a Gaussian distribution with zero mean and unit variance.

Note that the dynamics (1) is deterministic and is, moreover, intrinsically non-Hamiltonian. The latter is due to the quenched-disordered frequency term, which may be understood as follows. The ‘torque’ term due to interaction on the right-hand side of Eq. (1) may be obtained from a potential $\mathcal{V}(\{\theta_i\}) \equiv (K/2) \sum_{i,j=1}^N (a_{ij}/\kappa_i) [1 - \cos(\theta_i - \theta_j)]$, however, a similar procedure cannot be implemented for the frequency term. Although an ad hoc potential $\sim -\sum_{i=1}^N \omega_i \theta_i$ yields the frequency term, it would nevertheless not be periodic in the phases and thus fail to be a bona fide potential of the system. Thus the dynamics (1) cannot be interpreted as a Hamiltonian one describing overdamped motion on a potential landscape with $d\theta_i/dt = -\partial\mathcal{V}(\{\theta_i\})/d\theta_i$. Consequently, the dynamics (1) relaxes at long times to a nonequilibrium stationary state. As obvious from the above argument, for $\Delta = 0$, i.e., when the natural frequencies are identical ($\omega_i = \omega \forall i$), the dynamics indeed becomes Hamiltonian (as viewed from the co-moving frame) with the long-time dynamics reaching an equilibrium stationary state. This corresponds to values of θ_i that minimize the potential $\mathcal{V}(\{\theta_i\})$ [35].

Let us now briefly summarize the known results for the stationary state of the dynamics (1) in various limits. For $\sigma \leq 0$, the 1DLR3 network develops a finite spectral gap indicating spectral dimension $d_s = \infty$ [11, 36]. For $\sigma = -1$, $a_{ij} = 1 \forall i, j$, the dynamics reduces to that of a mean-field, *all-to-all* coupled model, originally introduced by Kuramoto [12]. Depending on the value of the coupling K , this model exhibits two qualitatively different phases in the thermodynamic limit: a low- K unsynchronized phase where the oscillators run incoherently (a more precise definition will be given in the following section) and a high- K synchronized phase where a macroscopic number of oscillators or even all of them lock their frequencies despite having different natural frequencies, and run coherently. The dynamics (1) exhibits a supercritical bifurcation between these two phases as one tunes K across a critical value K_c [12, 13, 35]. By analogy with a statistical system, we may associate the bifurcation behavior with a continuous phase transition [35, 37]. From now on, we use ‘‘phase transition’’ instead of ‘‘bifurcation’’ throughout this paper. One would expect a similar phase transition for $\sigma \leq 0$. On the other hand, in the opposite limit $\sigma \rightarrow \infty$, the dynamics is equivalent to that

on a one-dimensional chain with a nearest-neighbor interaction, which in the limit $N \rightarrow \infty$ does not exhibit any ordered phase at any K and hence no phase transition [13].

For $\sigma > 0$, the model has a finite spectral dimension: based on the study in Ref. [11], one expects $d_s = 1$ for $\sigma \geq 2$ and $d_s = 2/\sigma$ for $0 < \sigma < 1/3$, the same as on a fully connected weighted graph [36]. However, in the range $1/3 \leq \sigma < 2$, the behavior deviates from that of a fully connected weighted graph, and one needs to study the low-energy spectrum to determine d_s . In this context, we ask: What is the role of d_s on the synchronization dynamics of the Kuramoto model? How does the network disorder affect the dynamics? Or is the spectral dimension the only relevant parameter determining the universality of the dynamics on such a disordered graph? A thorough investigation to address these questions is one of the primary goals of the present work. A recent study in this direction can be found in Ref. [21], where the synchronization dynamics of the Kuramoto model was studied on a complex network manifold, which is different from ours.

As we will also investigate the role of d_s for the universality of the phase transition of the classical XY model, let us now summarize the known results for the XY model. Similar to the Kuramoto model, it does not exhibit any phase transition in the limit $N \rightarrow \infty$ on a 1D lattice with nearest-neighbor interactions, which corresponds to $\sigma \geq 2$ in our model. Note that on a two-dimensional regular lattice, this model undergoes the Berezinskii-Kosterlitz-Thouless (BKT) phase transition [38, 39]. Following the Mermin-Wagner theorem, the lower critical dimension for a phase transition is $d^l = 2$ [40]. A generalization of the Mermin-Wagner theorem for graphs states that spontaneous breaking of continuous symmetry is not possible on graph that is “recursive on average”, i.e., on a graph with “average spectral dimension” $d_s \leq 2$. Instead, it is possible only on a graph that is “transient on average” ($d_s > 2$) [16, 17]. The XY model on the Watts-Strogatz small-world network exhibits a mean-field type continuous phase transition. A study of the XY model on complex networks with an annealed network approximation shows the existence of a continuous phase transition with the critical temperature being proportional to the second moment of the degree distribution. This implies that the critical temperature is finite only if the second moment is finite [6].

There have been several recent works analyzing the fate of a BKT quasi-long range ordered phase in a long-range interacting system. The XY dynamics on a 2D long-range interacting systems, which could be thought of as an ‘annealed’ version of our model in 2D, where the interaction decays as $\sim |i - j|^{-(2+\sigma)}$, yields a rich phase diagram showing the existence of both conventional continuous and BKT transitions in the region $7/4 < \sigma < 2$, and belonging to the BKT universality class for $\sigma > 2$ [41]. Another recent study of the XY dynamics on a two-dimensional version of a variant of our

model, where the connection probability $\sim |i - j|^{-(2+\sigma)}$, verifies the theoretical prediction that the dynamics belongs to the BKT universality class for $\sigma \geq 2$ and exhibits a continuous phase transition for $\sigma < 2$ [26, 27]. Also, a BKT transition is predicted in the critical dynamics of the XY model on a 1D long-range power-law interacting system for $d_s = 2$ [42, 43].

The fact that the underlying topology of the network plays a crucial role in the critical dynamics and the advantage that one can realize spectral dimensions d_s lower than 2 in our 1DLR3 model motivate us to investigate the critical dynamics of the model on a network with $d_s = 2$. Investigating BKT on such a graph with 1D backbone would be a good test of the universality. Further, it would be interesting to see how the topological excitations, in case a quasi-ordered phase exists, are formed on such a network. This constitutes the second part of our work, where we explore the dynamics of the XY model on the 1DLR3 graph and test the theoretical prediction for the dependence of the universal behavior of BKT and conventional phase transitions on the spectral dimension.

III. LINEAR THEORY

In this section we first study the dynamics under linear approximation on a general network: $\sin(\theta_j - \theta_i) \approx (\theta_j - \theta_i)$, $\forall i, j$. This corresponds to the case of a very strong K value for the Kuramoto model, and very low-temperature for the XY model (see Sec. VI). The linearized equation, as obtained from Eq. (1), now reads as,

$$\frac{d\theta_i}{dt} = \omega_i - K \sum_{j=1}^N \mathcal{L}_{ij} \theta_j. \quad (2)$$

Here \mathcal{L}_{ij} , defined as

$$\mathcal{L}_{ij} := \delta_{ij} - \frac{a_{ij}}{\kappa_i}, \quad i, j = 1, 2, 3, \dots, N, \quad (3)$$

is the (i, j) -th element of the associated network Laplacian \mathcal{L} [7, 44]. Note that, by definition (3), the Laplacian \mathcal{L} is asymmetric; however, it can be shown easily that the eigenvalues $\{\lambda_i\}_{i=1,2,3,\dots,N}$ of \mathcal{L} are real and non-negative, with the smallest one being $\lambda_1 = 0$.

To analyze the dynamics (2), we work in the eigenbasis of the asymmetric Laplacian \mathcal{L} . If $|v_m^R\rangle$ and $\langle v_m^L|$ be the right and left eigenvectors corresponding to an eigenvalue λ_m , we can represent a state given by the phases of the oscillators, $|\theta\rangle = (\theta_1, \theta_2, \dots, \theta_N)^\top$, in an eigenbasis as follows:

$$|\theta\rangle = \sum_{m=1}^N \langle v_m^L | \theta \rangle |v_m^R\rangle = \sum_{m=1}^N \theta_{\lambda_m}^R |v_m^R\rangle, \quad (4)$$

$$\langle \theta | = \sum_{m=1}^N \langle \theta | v_m^R \rangle \langle v_m^L | = \sum_{m=1}^N \theta_{\lambda_m}^L \langle v_m^L |, \quad (5)$$

where $x_{\lambda_m}^R := \langle v_m^L | x \rangle$, and $x_{\lambda_m}^L := \langle x | v_m^R \rangle$. Similarly, a given realization of the natural frequencies ($\{\omega_i\}$) can also be represented by

$$|\omega\rangle = \sum_{m=1}^N \omega_{\lambda_m}^R |v_m^R\rangle, \quad \langle\omega| = \sum_{m=1}^N \omega_{\lambda_m}^L \langle v_m^L|. \quad (6)$$

Note that the Laplacian \mathcal{L} is now diagonalizable by the modal matrix \mathbf{P} as follows:

$$\mathbf{P}^{-1} \mathcal{L} \mathbf{P} = \mathbf{D}, \quad (7)$$

where \mathbf{D} is a diagonal matrix with elements being the eigenvalues of the Laplacian $0 = \lambda_1 < \lambda_2 \leq \lambda_3, \dots, \leq \lambda_N$. By construction, the right eigenvectors $|v_m^R\rangle$ form the columns of \mathbf{P} , whereas the left eigenvectors $\langle v_m^L|$ form the rows of \mathbf{P}^{-1} . These two sets of eigenvectors form a complete basis, are dual to each other, and can be normalized as $\langle v_m^L | v_{m'}^R \rangle = \delta_{m,m'}$. Moreover, normalization of the eigenvectors guarantees that $\mathbf{P}^{-1} \mathbf{P} = \mathbf{P} \mathbf{P}^{-1} = \mathbf{I}$.

A. Observables: Phase fluctuations and phase correlations

We compute two observables, namely, the average fluctuation of the phases and the phase correlation over the entire network, as proposed in Refs. [21, 45], to characterize the stability of the synchronized/ordered phase. The phase fluctuation is defined by

$$W^2 = \frac{1}{N} \left\langle \sum_{i=1}^N [\theta_i - \bar{\theta}]^2 \right\rangle = \langle \bar{\theta}^2 - \bar{\theta}^2 \rangle. \quad (8)$$

where $\bar{\theta} := (1/N) \sum_{i=1}^N \theta_i$, $\bar{\theta}^2 := (1/N) \sum_{i=1}^N \theta_i^2$ are the spatial averages, and $\langle \cdot \rangle$ denotes the average over realizations. We now express these spatial averages in the eigenbasis coefficients $\theta_{\lambda}^{L,R}$.

We denote $\theta_i = \langle i | \theta \rangle$, where $|i\rangle = (0, \dots, 0, i, 0, \dots, 0)_{\mathbf{I}_N}^T$. We thus have

$$\begin{aligned} \bar{\theta} &= \frac{1}{N} \sum_{i=1}^N \theta_i = \frac{1}{N} \sum_{i=1}^N \langle i | \theta \rangle = \frac{1}{N} \sum_{i=1}^N \sum_{m=1}^N \theta_{\lambda_m}^R \langle i | v_m^R \rangle \\ &= \frac{1}{N} \theta_{\lambda_1}^R \sum_{i=1}^N \langle i | v_1^R \rangle + \frac{1}{N} \sum_{m=2}^N \theta_{\lambda_m}^R \sum_{i=1}^N \langle i | v_m^R \rangle \end{aligned} \quad (9)$$

Similarly, we can express the average phase in the left eigenbasis and obtain

$$\begin{aligned} \bar{\theta} &= \frac{1}{N} \sum_{i=1}^N \langle \theta | i \rangle = \frac{1}{N} \sum_{m=1}^N \theta_{\lambda_m}^L \sum_{i=1}^N \langle v_m^L | i \rangle \\ &= \frac{1}{N} \theta_{\lambda_1}^L \sum_{i=1}^N \langle v_1^L | i \rangle + \frac{1}{N} \sum_{m=2}^N \theta_{\lambda_m}^L \sum_{i=1}^N \langle v_m^L | i \rangle. \end{aligned} \quad (10)$$

Next we will derive a few properties of the Laplacian \mathcal{L} to simplify the above averages. The fact that $\sum_{j=1}^N \mathcal{L} |j\rangle = 0$, implies

$$|v_1^R\rangle = \sum_{i=1}^N |i\rangle, \quad \text{corresponding to } \lambda_1 = 0. \quad (11)$$

Consequently,

$$\sum_{i=1}^N \langle v_m^L | i \rangle = 0, \quad \forall m \neq 1. \quad (12)$$

This result can also be understood from elementary theory of random walks [46] on a network, where the Laplacian \mathcal{L}^\top of Eq. (3) is the master operator or generator of the walk on the network.

Assuming this process to be ergodic, it has a unique stationary state which is given by $|v_1^R\rangle$ corresponding to $\lambda_1 = 0$. One can also show that the $\langle v_m^L|$ and $|v_m^R\rangle$ of \mathcal{L} are related through

$$|v_m^L\rangle = \mathcal{K} |v_m^R\rangle. \quad (13)$$

where $\mathcal{K} = \text{diag.}(\kappa_1, \dots, \kappa_N)$. It readily follows from Eqs. (11, 13) that

$$\langle v_1^L| = \frac{1}{\langle \kappa \rangle N} \sum_{i=1}^N \langle i | \kappa_i, \quad (14)$$

so that the orthogonality condition of the eigenvectors is satisfied. Here, $\langle \kappa \rangle = (1/N) \sum_{i=1}^N \kappa_i$. Using Eqs. (11, 12, 14), one obtains from Eqs. (9, 10), respectively,

$$\bar{\theta} = \theta_{\lambda_1}^R + \frac{1}{N} \sum_{m=2}^N \theta_{\lambda_m}^R \sum_{i=1}^N \langle i | v_m^R \rangle \quad \text{and} \quad \bar{\theta} = \frac{1}{N} \theta_{\lambda_1}^L. \quad (15)$$

When averaged over ensembles, we have

$$\langle \bar{\theta}^2 \rangle = \frac{1}{N} \langle \theta_{\lambda_1}^L \theta_{\lambda_1}^R \rangle + \frac{1}{N^2} \left\langle \sum_{m=2}^N \theta_{\lambda_1}^L \theta_{\lambda_m}^R \sum_{i=1}^N \langle i | v_m^R \rangle \right\rangle. \quad (16)$$

The second term on the right hand side of Eq. (16) will vanish at long times, which can be understood as follows: For any dynamics of type (2), where ω_i 's act as stochastic force, be it 'quenched' (e.g., when they act as natural frequencies in the Kuramoto model) or 'annealed' (e.g., when they represent Gaussian white noise), the evolution equations for $\theta_{\lambda_m}^{L/R}$ gets decoupled in the eigen basis of \mathcal{L} . The $\theta_{\lambda_m}^{L/R}$ can be thought of as velocities of Brownian particles with $\omega_{\lambda_m}^{L/R}$ being stochastic force and K_{λ_m} plays the role of damping constant; see Appendix A. Thus, at long times i.e. $t \rightarrow \infty$, the ensemble average $\langle \theta_{\lambda_m}^{L/R} \rangle$ will decay to zero for each m , except

for $m = 1$ for which $\lambda_1 = 0$, so long as the ensemble average of the stochastic force is zero, i.e., $\langle \omega_{\lambda_m}^{L/R} \rangle = 0$. Thus, in the limit $t \rightarrow \infty$, we have from Eq. (16),

$$\langle \bar{\theta}^2 \rangle = \frac{1}{N} \langle \theta_{\lambda_1}^L \theta_{\lambda_1}^R \rangle. \quad (17)$$

Now, the average squared phase, when expressed in eigenbasis,

$$\begin{aligned} \bar{\theta}^2 &= \frac{1}{N} \sum_{i=1}^N \theta_i^2 = \frac{1}{N} \langle \theta | \theta \rangle = \frac{1}{N} \sum_{m=1}^N \sum_{m'=1}^N \theta_{\lambda_m}^L \theta_{\lambda_{m'}}^R \langle v_m^L | v_{m'}^R \rangle \\ &= \frac{1}{N} \sum_{m=1}^N \theta_{\lambda_m}^L \theta_{\lambda_m}^R. \end{aligned} \quad (18)$$

We are interested in the phase fluctuations in the stationary state attained at long times. Thus, Eq. (8), on using Eqs. (17, 18), yields for the phase fluctuations in the stationary state,

$$W^2 = \langle \bar{\theta}^2 - \bar{\theta}^2 \rangle = \frac{1}{N} \left\langle \sum_{m=2}^N \theta_{\lambda_m}^L \theta_{\lambda_m}^R \right\rangle = \frac{1}{N} \sum_{m=2}^N \langle \theta_{\lambda_m}^L \theta_{\lambda_m}^R \rangle. \quad (19)$$

In the continuum limit, Eq. (19) can be expressed as

$$W^2 = \int_{\lambda_2}^{\lambda_{\max}} d\lambda \rho(\lambda) \langle \theta_{\lambda}^L \theta_{\lambda}^R \rangle, \quad (20)$$

where $\rho(\lambda)$ is the density of eigenvalues of the Laplacian \mathcal{L} , λ_2 denotes the first nonzero (Fiedler) eigenvalue. The quantity

$$\langle \theta_{\lambda}^L \theta_{\lambda}^R \rangle = \int_{-\infty}^{+\infty} \int_{-\infty}^{+\infty} d\theta_{\lambda}^L d\theta_{\lambda}^R \theta_{\lambda}^L \theta_{\lambda}^R P_{\text{st}}(\theta_{\lambda}^L, \theta_{\lambda}^R), \quad (21)$$

where $P_{\text{st}}(\theta_{\lambda}^L, \theta_{\lambda}^R)$ is the stationary joint probability distribution of θ_{λ}^L and θ_{λ}^R .

We now compute another important quantity, the phase correlation defined by [21]

$$C = \frac{1}{N} \langle \langle \theta | \mathcal{L} \theta \rangle \rangle, \quad (22)$$

where the outer brackets $\langle \cdot \rangle$ denote again the average over realizations. Expressing it in eigenbasis we obtain

$$\begin{aligned} C &= \frac{1}{N} \left\langle \sum_{m=1}^N \lambda_m \langle \theta | v_m^R \rangle \langle v_m^L | \theta \rangle \right\rangle = \frac{1}{N} \left\langle \sum_{m=1}^N \lambda_m \theta_{\lambda_m}^L \theta_{\lambda_m}^R \right\rangle \\ &= \frac{1}{N} \left\langle \sum_{m=2}^N \lambda_m \theta_{\lambda_m}^L \theta_{\lambda_m}^R \right\rangle = \frac{1}{N} \sum_{m=2}^N \lambda_m \langle \theta_{\lambda_m}^L \theta_{\lambda_m}^R \rangle, \end{aligned} \quad (23)$$

as $\lambda_1 = 0$. Thus at long times, in the continuum limit,

$$C = \int_{\lambda_2}^{\lambda_{\max}} d\lambda \lambda \rho(\lambda) \langle \theta_{\lambda}^L \theta_{\lambda}^R \rangle. \quad (24)$$

Note that the above expressions, given by Eq. (20, 24), are very general in the sense that they follow immediately from unique stationarity of the dynamics on the network. Thus, it holds for any dynamics occurring on the network so long as it reaches a unique stationary state.

Now, in a general network or disordered system, the density of low-lying eigenvalues $\rho(\lambda)$ of the network Laplacian follows the scaling [10]

$$\rho(\lambda) \sim \lambda^{d_s/2-1} \quad \text{for } \lambda \ll 1, \quad (25)$$

where d_s is the *spectral dimension* of the network. Furthermore, the smallest non-zero eigenvalue λ_2 follows the scaling with the network size N as

$$\lambda_2 \propto N^{-2/d_s}. \quad (26)$$

Equations (25,26) would help us express the quantities of interest as a function of the spectral dimension d_s .

In the following, we now proceed to compute the quantities W^2 and C explicitly for the Kuramoto and XY models, in order to estimate the lower critical dimension of the associated transitions.

B. Theoretical prediction for the Kuramoto model

In this section, we explicitly compute W^2 and C for the Kuramoto model and study their behavior with system size N , which in turn helps to estimate the lower critical dimension of the associated transitions. To start with, we first project the linearized Kuramoto dynamics (2) along the eigenbasis and obtain evolution equations for $\theta_{\lambda}^{L/R}$. One can then obtain for $P_{\text{st}}(\theta_{\lambda}^L, \theta_{\lambda}^R)$ by using the Fokker-Planck formalism, and substitute it in Eq. (21) to compute $\langle \theta_{\lambda}^L \theta_{\lambda}^R \rangle$. However, we compute $\langle \theta_{\lambda}^L \theta_{\lambda}^R \rangle$ directly using formal solutions as sketched in Appendix A. We have in the stationary state

$$\langle \theta_{\lambda}^L \theta_{\lambda}^R \rangle = \frac{1}{K^2 \lambda^2}, \quad (27)$$

which is substituted in Eq. (20) to arrive at

$$W^2 = \int_{\lambda_2}^{\lambda_{\max}} d\lambda \frac{\rho(\lambda)}{K^2 \lambda^2}. \quad (28)$$

Note that Eq. (20) and thus Eq. (28) was obtained in Ref. [21] from the explicit solution of the linearized Kuramoto model. However, since we have shown the generality of this equation in the previous section, we directly use it here to obtain the fluctuations.

Further, using Eq. (25) and Eq. (26), we finally obtain

$$W^2 \sim \begin{cases} N^{4/d_s-1}, & d_s < 4, \\ \ln N & d_s = 4, \\ \text{const.} & d_s > 4. \end{cases}$$

A stable synchronized phase requires the average phase fluctuations in the stationary state to be finite in the

thermodynamic limit, i.e., $W^2 < \infty$ as $N \rightarrow \infty$; otherwise, it becomes thermodynamically unstable. Thus, it immediately follows from Eq. (29) that the lower critical dimension for the phase synchronization transition in the Kuramoto model is $d_s = 4$.

On the other hand, using Eq. (27) we obtain from Eq. (24) for the stationary-state phase correlations

$$C = \int_{\lambda_2}^{\lambda_{\max}} d\lambda \frac{\rho(\lambda)}{K^2 \lambda}, \quad (29)$$

yielding

$$C \sim \begin{cases} N^{2/d_s-1}, & d_s < 2, \\ \ln N & d_s = 2, \\ \text{const.} & d_s > 2. \end{cases} \quad (30)$$

The correlation function C essentially represents the mean-square phase difference between the nearest-neighbor oscillators in the network. Thus, a divergence in C implies that the average nearest-neighbor phase difference diverges, which contradicts the very assumption of the linear theory. In other words, the linear approximation becomes invalid in this case.

The correlation C provides useful information about the entrainment dynamics. Physically, an entrained phase is possible so long as the average nearest-neighbor phase difference is small, i.e., the linear theory is valid. Thus, one obtains about the possibility of an entrained phase from the finiteness of C . Based on this, it follows from Eq. (30) that entrainment in the Kuramoto model is possible only if the spectral dimension $d_s > 2$.

C. Theoretical prediction for the XY model

In this section, we study the system-size behavior of W^2 and C for the dynamics of classical XY model; see Sec VI for model definition and detailed discussion on the XY model. Following a similar approach as for the Kuramoto model, for the linearized dynamics of the XY-model projected onto the eigenbasis, one arrives in the stationary state

$$\langle \theta_\lambda^L \theta_\lambda^R \rangle = \frac{T}{K\lambda}. \quad (31)$$

A detailed derivation is provided in Appendix A.

On substituting Eq. (31) into Eq. (20), we obtain the phase fluctuations of the XY model as

$$W^2 = \int_{\lambda_2}^{\lambda_{\max}} d\lambda \rho(\lambda) \frac{T}{K\lambda}. \quad (32)$$

Using Eqs. (25) and (26), one obtains from Eq. (32) for the stationary-state fluctuations

$$W^2 \sim \begin{cases} N^{2/d_s-1}, & d_s < 2, \\ \ln N & d_s = 2, \\ \text{const.} & d_s > 2. \end{cases} \quad (33)$$

Note that the functional dependence of W^2 for the XY model and C of the Kuramoto model on the eigenvalue spectra of the associated network is the same. Based on the discussion in the previous section, it follows from Eq. (33) that a thermodynamically stable ordered phase is possible only in $d_s > 2$, and the marginal case $d_s = 2$ marks the lower critical dimension.

The correlation in the XY model,

$$C = \int_{\lambda_2}^{\lambda_{\max}} d\lambda \rho(\lambda) \frac{T}{K} = \frac{T}{K}, \quad (34)$$

is a constant for any $T, K > 0$ and $d_s < \infty$. It implies that the linear theory is always valid. This can be understood physically as follows: Since the XY spins are equivalent to Kuramoto oscillators with identical natural frequencies, the fluctuation in the phase-velocity is always zero, thereby they are inherently always ‘entrained’. This is why only the phase transition is discussed in the context of the XY model. The behavior of C obtained in Eq. (34) is thus consistent with the expected properties of the XY model.

Note that the linear theory never suggests the existence of a phase or entrainment transitions in any d_s , for any temperature T , or coupling strength K . It only states that if an ordered/synchronized state is possible, whether this state would be stable or not. A disordered/unentrained phase emerges and hence, a phase transition actually occurs due to the nonlinearity present in the dynamics. In the following section, we therefore study the nonlinear system numerically and test our theoretical prediction for both the Kuramoto and XY models to understand the role of spectral dimension and network disorder in them.

Further, in numerics we tune the network parameter σ to realize various spectral dimensions d_s . The relation between σ and d_s for our network is nontrivial. It agrees well, and is thus given by $d_s = 2/\sigma$ and $d_s = 1$ for small σ ($\sigma < 1/3$) and large σ ($\sigma > 2$) respectively, with that of the fully connected 1D weighted graph, where the weight factor between two sites (i, j) is $\sim d_{ij}^{-(1+\sigma)}$ with d_{ij} being the Euclidean shortest distance between the sites (i, j) on the graph. For the intermediate values of σ , one needs to numerically compute d_s from finite-size scaling of low-lying eigenvalues of the graph Laplacian. The dimensions $d_s = 4$ and 2 correspond to approximately $\sigma = 0.5$ and 0.875, respectively; see Ref. [11] and Fig. 4.

IV. NUMERICAL STUDY: OBSERVABLES

We are interested in studying two types of synchronizations: phase synchronization and frequency entrainment.

The various statistical quantities that we measure in our study are as follows:

A. Order parameter

To measure frequency entrainment, we introduce the Edwards-Anderson order parameter, defined as [47]

$$r_{EA} e^{i\psi_{EA}} \equiv \lim_{T \rightarrow \infty} \frac{1}{N} \sum_{j=1}^N e^{i[\theta_j(t_0+T) - \theta_j(t_0)]}, \quad (35)$$

where t_0 is the time larger than the initial transient time so that the dynamics settles down into a stationary state. The quantity r_{EA} ($0 \leq r_{EA} \leq 1$) measures the amount of entrainment present in the system; $r_{EA} = 1$ corresponds to a fully entrained phase, whereas $r_{EA} = 0$ corresponds to an unentrained phase. Note that by ‘entrainment’, we mean the oscillators’ stationary-state long-time average of the frequencies to be the same but not necessarily their instantaneous frequencies.

To study the phase synchronization, let us also introduce the Kuramoto synchronization order parameter [12, 13]

$$r(t) e^{i\psi(t)} \equiv \frac{1}{N} \sum_{j=1}^N e^{i\theta_j(t)}, \quad (36)$$

where the quantity r ($0 \leq r \leq 1$) measures the amount of global phase synchrony present in the system at a given instant in time t , while $\psi \in [0, 2\pi)$ measures the average phase at that instant [13].

B. Dynamic fluctuations

We study the behavior of the stationary-state fluctuations of the frequency order parameter by measuring the quantity

$$\chi = N [\langle r_{EA}^2 \rangle - \langle r_{EA} \rangle^2]. \quad (37)$$

In our simulations, to compute the frequency order parameter for a given realization of the dynamics, we first evolve the dynamics until it reaches a stationary state, signaled by a stationary distribution of the phase order parameter. In the stationary state, we choose time intervals of varying lengths $T_n = T + n\Delta T$, with $T = 500$, $\Delta T = 10$, and n running from $0, 1, 2, \dots, 199$, to construct a distribution of the EA order parameter, the mean of which yields the time-averaged EA order parameter. The quantity thus computed is further averaged over many such realizations of the network and natural frequencies of the oscillators (sample average). Here, $\langle \cdot \rangle$ and $[\cdot]$ represent the time average in the stationary state and sample averages, respectively. This quantity is equivalent to the susceptibility in statistical systems. We note that in computing the time average, it is advisable

to choose non-overlapping time intervals when constructing the distribution in order to eliminate any statistical correlations in the data. Clearly, this approach is computationally very expensive. However, once averaged over a long total time, we have observed that both of these schemes yield qualitatively similar behavior.

A similar quantity for the stationary-state fluctuations of the phase order parameter is measured as follows

$$\chi = N [\langle r^2 \rangle - \langle r \rangle^2]. \quad (38)$$

Here, to compute the time-average value for a given realization of the dynamics, unlike in the previous case, one records only the values of phase order parameter at various time instants in the stationary state.

C. Binder Cumulant

To understand the existence as well as the nature of a phase transition, we consider another useful thermodynamic quantity, namely, the fourth-order Binder cumulant, defined on system of size N by [48, 49]

$$U = 1 - \left[\frac{\langle r^4 \rangle}{3\langle r^2 \rangle^2} \right], \quad (39)$$

where $\langle \cdot \rangle$ and $[\cdot]$ represent the time average in the stationary state and the sample average, respectively. We replace r in Eq. (39) by r_{EA} to study frequency entrainment dynamics.

Our analysis is based on the finite-size scaling hypothesis and we assume that this scaling holds also for continuous transitions in a nonequilibrium system, in particular for a large network in the limit $N \rightarrow \infty$. Then U converges to the asymptotic value $2/3$ in the ordered (entrained/synchronized) phase and to $1/3$ in the disordered (unentrained/unsynchronized) phase. For large but finite N the correlation length $\xi \ll N$ remains limited in both phases. Consequently, U for networks of various sizes N remains close to the aforementioned asymptotic values.

Now, in a continuous entrainment/phase transition, at criticality $\xi \gg N$, the system is expected to remain close to another fixed-point value U^* , independent of N . So, a feature of a continuous transition is hinted at by the existence of a common intersection point of the curves for U vs. the relevant coupling or noise strength for a network of various sizes N . The common intersection point corresponds to the critical parameter value of the transition at which fluctuation diverges and hence $\xi \rightarrow \infty$. However, in practice, due to statistical uncertainties, instead of a common intersection point, the curves may cross each other within a range of parameter values. To estimate the ‘‘true’’ critical parameter, one then needs to study a large system size, perform sample averaging and take into account finite-size effects. However, in our present work, our aim is not to estimate the critical point, but to investigate the very existence of a transition, if any. Data of numerical results reported in Sec V and Sec. VI

are obtained by numerically integrating the corresponding deterministic (Kuramoto model) and stochastic (XY model) governing dynamics employing the Runge-Kutta4 (RK4) and Euler-Maruyama algorithm respectively, with integration time step $dt = 0.01$.

V. RESULTS: UNIVERSALITY OF PHASE AND ENTRAINMENT TRANSITION

A. Frequency entrainment transition

With the observables mentioned above, we now proceed to study the entrainment dynamics in the Kuramoto model on networks of various spectral dimensions. Figure (1) shows the behavior of the stationary-state EA order parameter r_{EA} [panels (a-d)], dynamical fluctuations χ [panels (e-h)], and Binder cumulant U [panels (i-l)] as a function of coupling strength K for various σ values on networks of various sizes N .

For all σ values [panels (a-d)], the EA order parameter increases from small values $\mathcal{O}(1/\sqrt{N})$ to large values $\mathcal{O}(1)$. However, to investigate whether these unambiguously correspond to an entrainment transition in the thermodynamic limit, we study the behavior of dynamical fluctuations [panels (e-h)] and Binder cumulant U [panels (i-l)]. The divergence in χ at criticality in the thermodynamic limit is reflected in finite systems as a peak in the fluctuation curve, which is rounded at finite size. We further expect χ to be $\mathcal{O}(1)$ both in the ordered and disordered phase, in a region away from criticality. We call the parameter value at which the peak occurs a pseudo-critical point. A few comments on the Fig. 1(e-h) are in order: first, the peak height of χ increases with N ; second, the fluctuation curves look asymmetric around their maxima, and thus they are expected to yield two different values of the critical exponent corresponding to either side of the transition. This may be due to the heterogeneity present in our system: in our model, each oscillator experiences a different field due to its own intrinsic frequency and different degree. Thus, the usual renormalization group argument for equal exponents above and below the transition based on a few relevant variables may not work in such a case. Third, the fluctuation curves around the peak in the region of high K values become steeper as N increases. All these observations hint towards the existence of a transition.

At this point, a close scrutiny shows something very interesting. One expects, in general, the fluctuation curves around the peak in the region of high K value to be steeper as N increases, which implies diverging fluctuations only at the critical point and zero fluctuations away from criticality in the thermodynamic limit. This is indeed observed in panels (e-f), which correspond to $\sigma = 0.2$ and 0.4 , or equivalently, $d_s = 10$ and 5 . These bear a clear signature of an entrainment transition in the limit $N \rightarrow \infty$, as expected. However, for $\sigma \geq 0.6$ or $d_s \lesssim 3.33$ the behavior changes, see pan-

els (g-h) for $\sigma = 0.6$ and 0.8 , or equivalently, $d_s \approx 3.3$ and 2.5 . The curves broaden and imply large fluctuations that increase with N even for very large K away from pseudo-criticality; this precludes the existence of an ordered/entrained phase at high K in the thermodynamic limit. This shows that there is no entrained phase, and hence no entrainment-unentrainment transition for $\sigma \geq 0.6$, or $d_s \lesssim 3.33$.

To confirm this observation, we further look at the behavior of the Binder cumulant U [see Fig. 1(i-l)] as a function of coupling strength K for the same σ values. As observed in panel (i), the curves for various N intersect within a certain range of K ; also in panel (j), the behavior of U for the two largest networks $N = 2048$ and 4096 shows an intersection in U for large K that indicates an entrainment transition. Qualitatively different behavior is seen in panels (k) and (l), i.e. for $d_s \lesssim 3.33$, where the curves for different N do not intersect. This validates our observation, as obtained from the study of dynamic fluctuations.

We note that linear theory predicts the lower critical dimension the entrainment transition as $d_s = 2$, given that the correlation does not diverge. Here, we observe the absence of entrainment even in dimensions ($d_s \lesssim 3.33$) higher than the critical one. We believe this happens because of an enhanced fluctuations arising from the nontrivial interplay between the ‘quenched’ network disorder and the quenched frequency disorder, besides the nonlinearity in the dynamics, suppressing the entrained phase predicted from linear theory in this region.

B. Phase synchronization transition

In this section, we study the phase synchronization dynamics of the Kuramoto model on our network of various spectral dimensions and investigate the critical dimension to observe the phase transition. Figure 2 shows the behavior of the stationary-state Kuramoto order parameter r [panels (a-d)], dynamical fluctuations χ [panels (e-h)], and Binder cumulant U [panels (i-l)] as a function of coupling strength K for various σ values on networks of various sizes N .

Similar to the entrainment case, for all σ values [panels (a-d)], the Kuramoto order parameter also increases from small values $\mathcal{O}(1/\sqrt{N})$ to large values $\mathcal{O}(1)$. The behavior of the dynamic fluctuations of the Kuramoto order parameter for $\sigma = 0.2$ and 0.4 , or, equivalently, $d_s = 10$ and 5 [panels (e-f)] shows the existence of a phase synchronization transition in the limit $N \rightarrow \infty$. The case for $\sigma = 0.5$, which corresponds to $d_s = 4$ [panel (g)], is the marginal case as predicted from the linear theory; furthermore, panel (h) shows the behavior at $\sigma = 0.6$, or $d_s \approx 3.33$. In the latter two cases, the peaks of the fluctuation curves start to broaden for larger system size N in the region of high K , and thus imply large fluctuations in the thermodynamic limit. Thus, in the region

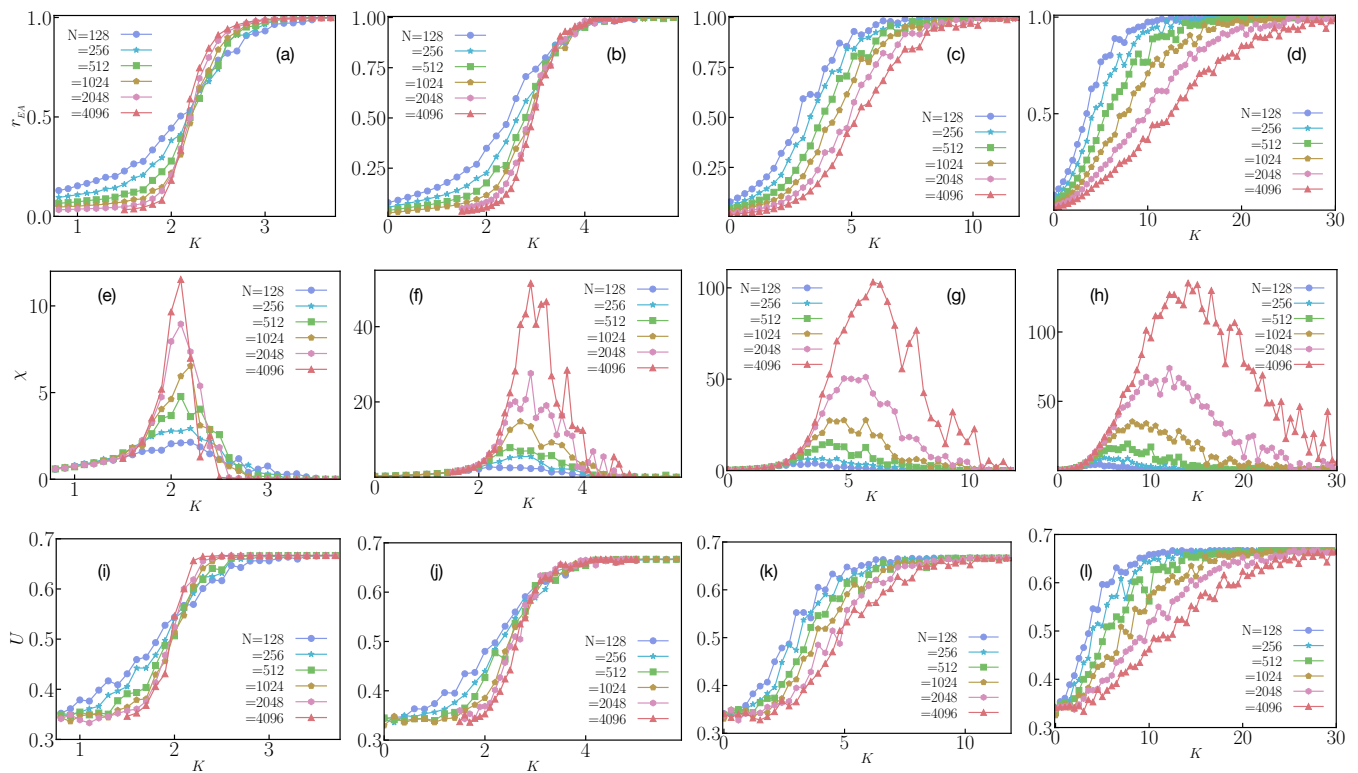


FIG. 1. Entrainment in Kuramoto dynamics: Stationary-state Edwards-Anderson order parameter r_{EA} [panels (a-d)], dynamical fluctuations χ [panels (e-h)], and Binder cumulant U [panels (i-l)] as a function of coupling strength K for 4 different σ values: $\sigma = 0.2$ [panels (a), (e), (i)], 0.4 [panels (b), (f), (j)], 0.6 [panels (c), (g), (k)] and 0.8 [panels (d), (h), (l)]. Data in each panel are obtained in the nonequilibrium stationary state by integrating the dynamics (1) on networks of sizes $N = 128, 256, 512, 1024, 2048,$ and 4096 as indicated in the legend and averaged over 50 different realizations of the network and intrinsic frequencies of the oscillators.

$\sigma \geq 0.5$ ($d_s \leq 4$), the broadening of the peak supports having no synchronized phase at any high K , and thus no phase synchronization-desynchronization transition.

This observation is further confirmed from the behavior of the Binder cumulant U [Fig. 2 (i-l)] as a function of coupling strength K : the curves for various sizes N cross in panels (i) and (j), which corresponds to $d_s = 10$ and 5, respectively. However, having no common intersection point among the various curves of U in panels (k) and (l) bears a clear signature of no phase synchronization transition for $\sigma \geq 0.5$, i.e. $d_s \leq 4$.

Our observation of the lower critical dimension of the phase synchronization transition is thus consistent with the prediction of linear theory in that the transition occurs only in $d_s > 4$. One may thus conclude that the network disorder does not affect the critical dynamics of the phase synchronization transition.

VI. XY MODEL LIMIT: UNIVERSALITY OF PHASE AND BKT TRANSITIONS

So far, our study focuses on the role of network disorder on the emergent dynamics of a non-equilibrium system.

At this point, we feel it worthwhile to explore its effect on the equilibrium dynamics. To this end, we consider the equilibrium limit of the dynamics (1), namely, the XY model limit. As already predicted by the linear theory, the lower critical dimension for a phase transition in the XY model on a general network is $d_s^l = 2$. We aim to verify in this section the universality of this phenomenon. The XY model is obtained from the Kuramoto model when the intrinsic frequencies of the oscillators are chosen to be identical, and moreover, is set to zero, and then subject to Gaussian white noise [18, 19]. The phase evolution equation now reads as

$$\frac{d\theta_i}{dt} = \frac{K}{\kappa_i} \sum_{j=1}^N a_{ij} \sin(\theta_j - \theta_i) + \eta_i(t), \quad (40)$$

where the term $\eta_i(t)$ is a Gaussian white noise characterized by

$$\langle \eta_i(t) \rangle = 0 \text{ and } \langle \eta_i(t) \eta_j(t') \rangle = 2T \delta_{ij} \delta(t - t'). \quad (41)$$

Here $\langle \cdot \rangle$ denotes averaging over noise realizations, and T is the noise strength proportional to the temperature of the system. One may view the system of identical oscillators to be in contact with a heat bath which is at a

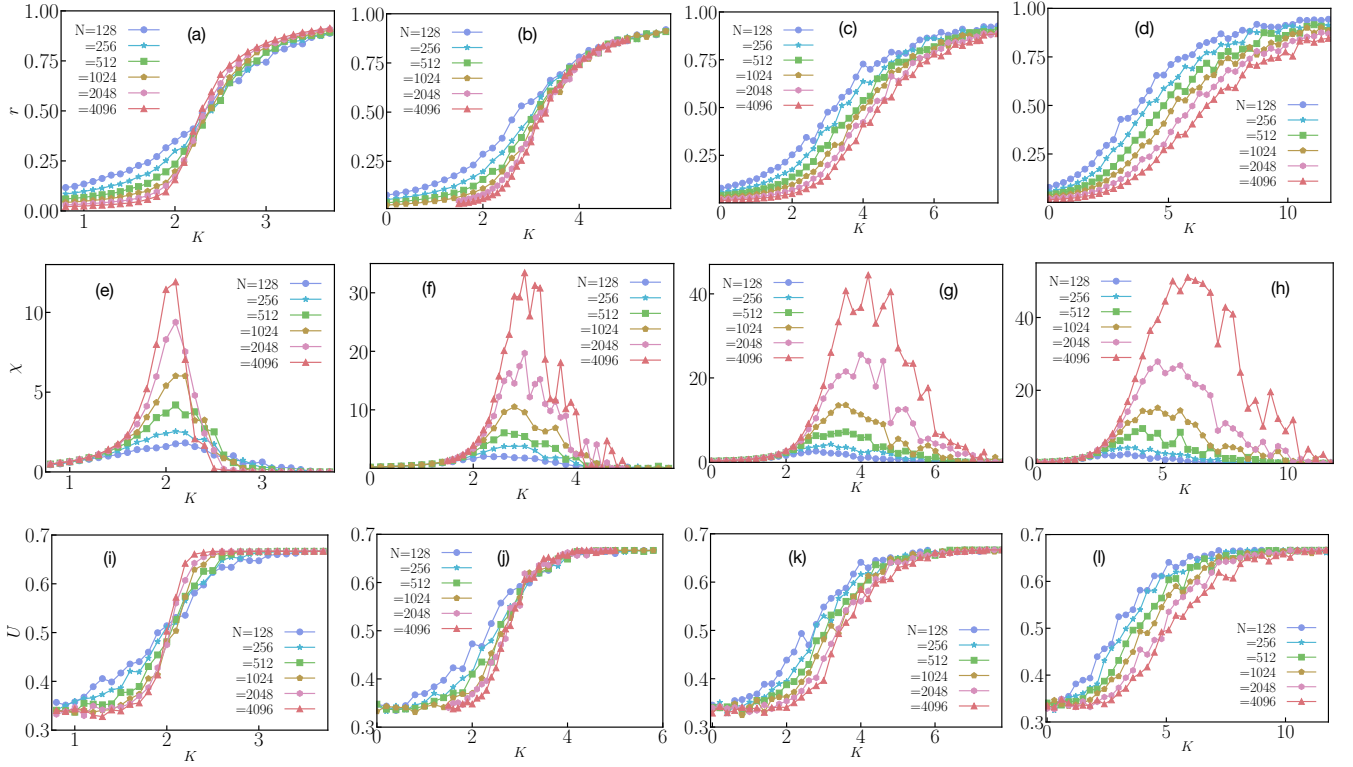


FIG. 2. Phase synchronization in Kuramoto dynamics: Stationary-state Kuramoto order parameter [panels (a-d)], dynamical fluctuations χ [panels (e-h)], and Binder cumulant U [panels (i-l)] as a function of coupling strength K for four different σ -values, namely, $\sigma = 0.2$ [panels (a), (e), (i)], 0.4 [panels (b), (f), (j)], 0.5 [panels (c), (g), (k)] and 0.6 [panels (d), (h), (l)]. Data in each panel are obtained in the nonequilibrium stationary state by integrating the dynamics (1) on networks of sizes $N = 128, 256, 512, 1024, 2048,$ and 4096 as indicated in the legend and averaged over 50 different realizations of the network and intrinsic frequencies of the oscillators.

temperature T . To show the explicit T dependence, one could write Eq. (40) as

$$\frac{d\theta_i}{dt} = \frac{K}{\kappa_i} \sum_{j=1}^N a_{ij} \sin(\theta_j - \theta_i) + \sqrt{2T} \zeta_i(t), \quad (42)$$

with

$$\langle \zeta_i(t) \rangle = 0 \text{ and } \langle \zeta_i(t) \zeta_j(t') \rangle = \delta_{ij} \delta(t - t'). \quad (43)$$

For $K \neq 0$ the equation of motion (42) can be brought into dimensionless form by the transformation $t \rightarrow Kt$, $g \rightarrow \sqrt{2T/K}$ and $\zeta_i(t) \rightarrow \zeta_i(t)/K$,

$$\frac{d\theta_i}{dt} = \frac{1}{\kappa_i} \sum_{j=1}^N a_{ij} \sin(\theta_j - \theta_i) + g \zeta_i(t). \quad (44)$$

The dynamics relaxes at long times to an equilibrium stationary state governed by Gibbs-Boltzmann statistics. The Kuramoto phase-order parameter r is now equivalent to the magnetization in a spin model of statistical physics. Note that, for convenience, all numerical results in this section are presented as a function of the reduced noise strength g that depends on the temperature T as $g = \sqrt{2T/K}$. However, we use both the terms

‘reduced noise strength’ and ‘temperature’ interchangeably throughout the text.

A. Phase transition

To study the phase transition, similar analysis of the various statistical quantities as in the previous sections is pursued, and is shown in Figure 3. The stationary-state phase order parameter [panels (a-d)] shows a transition as temperature increases in r -value from $\mathcal{O}(1)$ to $\mathcal{O}(1/\sqrt{N})$ on finite networks of size N . The behavior of fluctuations that the increase in peak height with N , and especially, that the fluctuation curves become steeper near pseudo-criticality in the region of the ordered phase, shows the existence of a phase transition for $\sigma = 0.1$ and 0.5 , i.e., $d_s = 20$ and 4 [panels(e-f)]. However, as $\sigma \geq 0.7$, e.g., in panels (g,h) corresponding to $\sigma = 0.7$ and $\sigma = 0.8$, or equivalently $d_s \approx 3$ and 2.5 , the maximum fluctuations appear to saturate with system size N (see insets). Also, the curves broaden with increasing N near their maxima in the region of the ordered phase, probably caused by strong finite size effects that hinder the realization of the ordered phase, whose existence has been proven in the

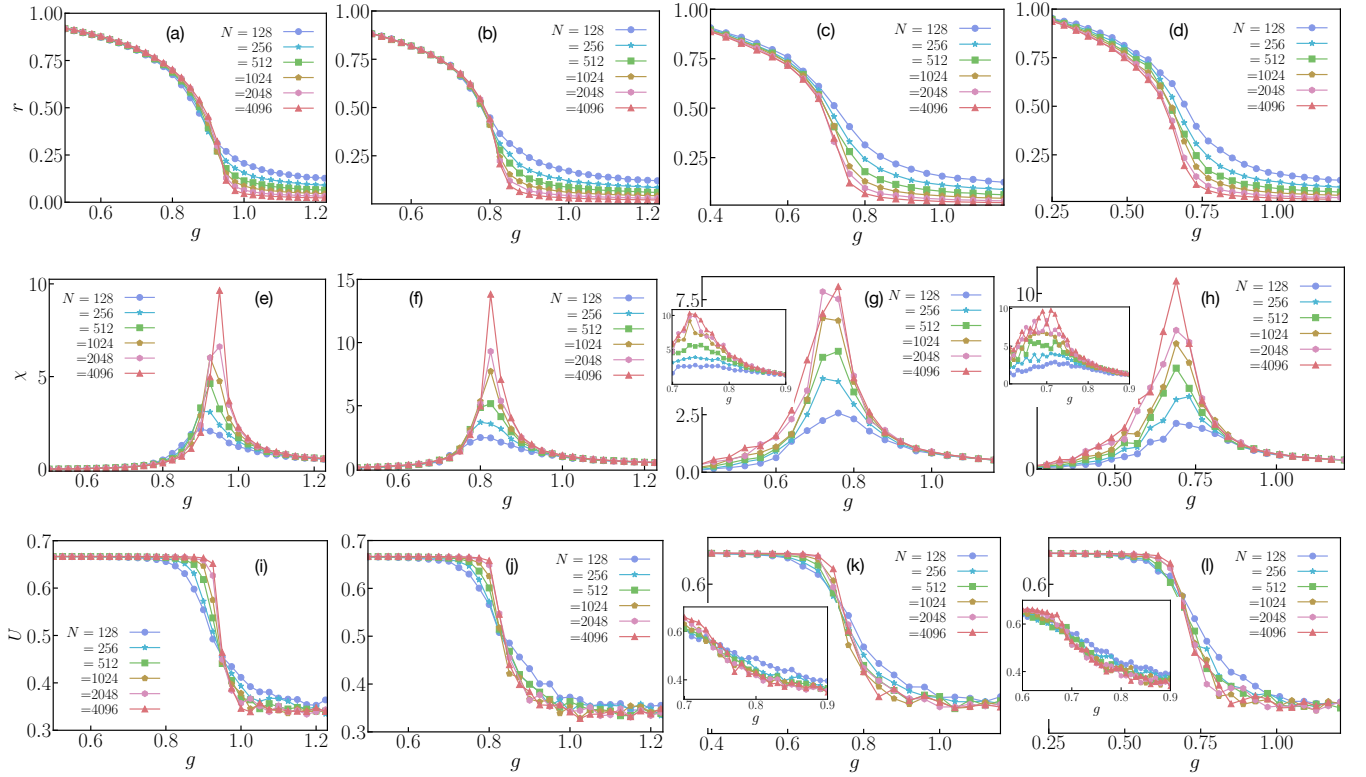


FIG. 3. XY model: Stationary-state phase order parameter r [panels (a-d)], dynamical fluctuations χ [panels (e-h)], and Binder cumulant U [panels (i-l)] as a function of noise strength $g = \sqrt{2T/K}$ for four different σ values, namely, $\sigma = 0.1$ [panels (a), (e), (i)], 0.5 [panels (b), (f), (j)], 0.7 [panels (c), (g), (k)] and 0.8 [panels (d), (h), (l)]. Data in each panel are obtained in the equilibrium stationary state by integrating the dynamics (44) on networks of sizes $N = 128, 256, 512, 1024$, and 2048 as indicated in the legend and averaged over 50 different realizations of the network and noise.

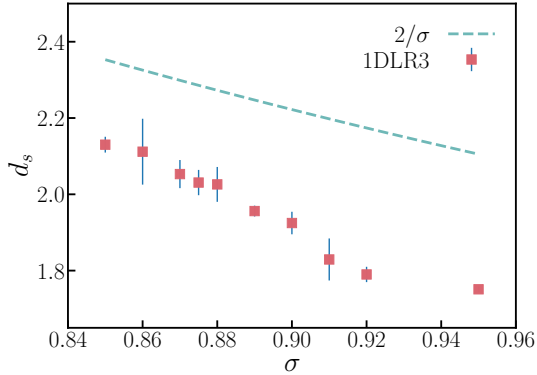


FIG. 4. Spectral dimension d_s as a function of σ of the 1DLR3 network as obtained by the finite-size scaling of the graph Laplacian spectrum. The dashed blue line represents the analytical expectation for a long-range weighted lattice.

thermodynamic limit [20]. Further, we show the behavior of the Binder cumulant U in Fig. 3(i-l) for the same σ values. The curves of U vs. g for various N seem to intersect clearly for $\sigma = 0.1$ and 0.5 [panels (i) and (j)], whereas for $\sigma = 0.7$ and 0.8 [panels (k) and (l)] their N -dependent behavior in the region of the ordered phase

does not show a clear intersection, consistent with our previous observation from dynamic fluctuations. Thus, in the region $\sigma \gtrsim 0.7$, i.e. $d_s \lesssim 3$, we do not obtain a clear signature of a phase transition. The missing evidences for the ordered phase in $d_s \lesssim 3$ ought to be the result of the strong finite-size effects generated by disorder as the model has been theoretically shown to magnetize in the thermodynamic limit for all $d_s > 2$ [20].

B. Fate of the *BKT* transition

So far, our study focused on the existence of a conventional phase transition on a network. This section is devoted to studying the Berezinskii-Kosterlitz-Thouless (*BKT*) transition on networks [38, 39]. As stated earlier, the Mermin-Wagner theorem states for an equilibrium system that a continuous symmetry cannot be broken spontaneously at any finite temperatures in spatial dimensions two or lower [40]. The 2D *XY* model exhibits an unconventional phase transition, the *BKT* transition, between a low-temperature quasi-ordered phase and high-temperature disordered phase [38, 39]. The quasi long-range ordered phase is characterized by an algebraic decay of correlations (infinite correlation length and di-

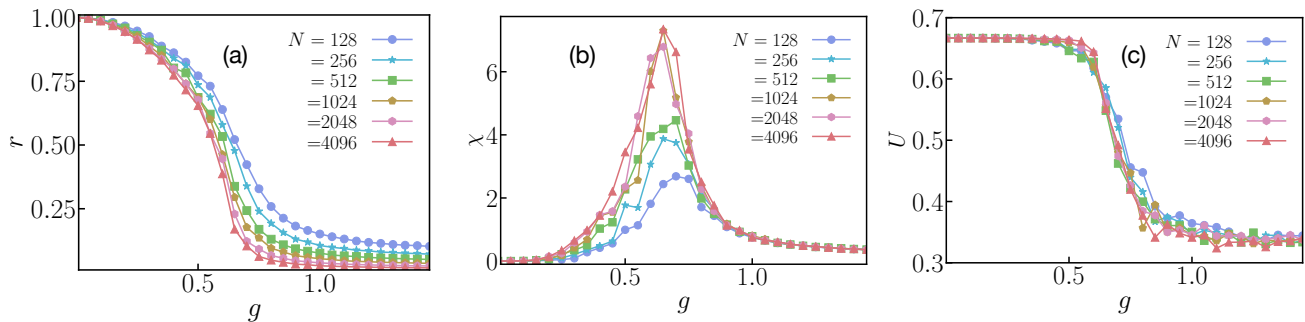


FIG. 5. BKT transition in XY model: Stationary-state phase order parameter r [panels (a)], dynamical fluctuations χ [panels (b)], and Binder cumulant U [panels (c)] as a function of reduced noise strength g for $\sigma = 0.875$ that corresponds to $d_s \approx 2.0$. Data in each panel are obtained in the equilibrium stationary state by integrating the dynamics (44) on networks of sizes $N = 128, 256, 512, 1024, 2048,$ and 4096 as indicated in the legend and averaged over 50 different realizations of the network and noise.

verging susceptibility), whereas the decay is exponential in the disordered phase. A generalization of the Mermin-Wagner theorem is as follows: No spontaneous breaking of continuous symmetry is possible on a “recursive on the average” graph, i.e. on a graph with “average spectral dimension” $d_s \leq 2$. The continuous symmetry models always have a broken symmetry phase at a finite temperature on the “transient on the average” graph ($d_s > 2$). Note that this is consistent with our theoretical prediction for the linear model.

Motivated by this, we ask if the XY dynamics on 1DLR3 network with $d_s = 2$ shows a BKT transition. In order to realize $d_s = 2$ with our network, we numerically compute d_s from finite-size scaling of low-lying eigenvalues of the graph Laplacian for various σ , which yields $\sigma = 0.875$ corresponding to $d_s \approx 2.03$; see Fig. 4. The behavior of various statistical quantities measured in the stationary state at this parameter value is shown in Fig. 5.

Now, for a system exhibiting a BKT transition at critical temperature T_{BKT} , in the region $T \leq T_{BKT}$, fluctuations diverge, and consequently the correlation length $\xi(N \rightarrow \infty)$ is infinite. Thus, for large but finite N , one would expect the fluctuations to scale with N at and below T_{BKT} . Also, the curves of U for various N are expected to stay close to a fixed point U^* in this region. However, in practical application, due to the statistical uncertainties, it is observed that T_{BKT} is very close to the point where the curves of U for various N begin to separate from the low- T asymptotic value [50].

Figure 5(a) shows the behavior of the stationary order parameter r as a function of noise strength g , which crosses over from low-temperature high r -value to a high temperature low r -value, typical of finite-size rounding of a sharp transition. However, as shown in panel (b), the fluctuations in the low-temperature region do not seem to increase with N (even the peak heights seem to get saturated) for high values of N , showing no divergence in this region in the thermodynamic limit. This is further confirmed by the behavior of the Binder cumulant

U [panel (c)]: the curves of U for various N do not seem to stay collapsed and then begin to separate from a low- g asymptotic value, nor even do they intersect clearly. This evidence speaks against a BKT transition in disordered graphs with $d_s = 2$; instead, its behavior is similar to that observed for $\sigma = 0.7$ and 0.8 ($d_s > 2$).

Based on these observations, we anticipate that the network disorder plays a crucial role in $0.6 < \sigma < 0.875$, or approximately, in spectral dimension $2 \leq d_s \lesssim 3$. The structural heterogeneity due to the presence of the long-range links acts as a source of quenched disorder. The lower critical dimension of the phase synchronization transition is $d_s = 4$, and in such high dimension the disorder fluctuation decreases with system sizes very fast, and the system becomes asymptotically homogeneous at large length scales, suppressing the fluctuations. Thus, the critical behavior of the phase synchronization transition in such disordered systems remains unaffected and is identical to that of the clean system. In contrast, for both the entrainment dynamics of the Kuramoto model and the phase transition of the XY model, the lower critical dimension is $d_s = 2$. In $2 \leq d_s \lesssim 3$, we believe that such a weak disorder makes the finite-size effects very strong, introducing enhanced fluctuations that vanish extremely slowly in the thermodynamic limit. Thus, the system remains inhomogeneous even at large length scales (for the system sizes we considered), making it extremely difficult to probe the existence of the ordered phase predicted by the linear theory and also by rigorous mathematical arguments [20]. However, a complete confirmation of this calls for an independent study.

VII. CONCLUSION

In this work, we have systematically investigated the role of spectral dimension d_s as a control parameter in determining the universality of phase transitions on a network. As a network, we employ a 1DLR3 graph on top of which we study two paradigmatic models: One

is the non-equilibrium dynamics of the Kuramoto model of synchronization, and the other one is the equilibrium dynamics of the classical XY model. To summarize our findings,

1. We have developed for a given dynamics occurring on the network, under linear approximation, a general relationship between stationary-state properties of the dynamics occurring on the network and the underlying network structures in terms of the density of eigenvalues of the network Laplacian. Our method is general in that it applies to both deterministic and stochastic dynamics on the network so long as it has a unique stationary state.
2. The linear theory predicts the lower critical spectral dimension for entrainment and synchronization transition in the Kuramoto model as $d_s = 2$ and $d_s = 4$, respectively, whereas, for the phase transition in the XY model, it yields $d_s = 2$.
3. Our detailed numerical investigation agrees well with the theoretical prediction of phase synchronization transition in the Kuramoto model. However, it does not yield a clear signature of entrainment transition in the Kuramoto model and phase transition in the XY model in $2 \leq d_s \lesssim 3$.

We thus anticipate that the quenched network disorder arising from the structural heterogeneity is harmless in spectral dimension $d_s > 3$ and the critical behavior in such disordered systems is identical to that of the clean system. However, for $2 \leq d_s \lesssim 3$ the disorder average introduces finite-size scaling contributions which vanish extremely slowly (possibly logarithmically) in the thermodynamic limit, making it extremely hard to probe the existence of the ordered phase predicted by the linear theory as well as by rigorous mathematical arguments [20]. Moreover, given the role of network disorder near $d_s = 2$, an immediate question arises: How can one realize a BKT transition in the dynamics of XY model on such a disordered system? A complete confirmation of such a nontrivial behavior and an answer to the imposed query require an independent study. Investigation in this direction is going on and will be reported elsewhere.

ACKNOWLEDGMENTS

We acknowledge fruitful discussions with Giacomo Gori. This project is supported by the Deutsche Forschungsgemeinschaft (DFG, German Research Foundation) under Germany's Excellence Strategy EXC 2181/1-390900948 (the Heidelberg STRUCTURES Excellence Cluster). M.S. also acknowledges support by the state of Baden-Württemberg through bwHPC cluster.

Appendix A: Linear theory: Derivation of $\langle \theta_\lambda^L(t) \theta_\lambda^R(t) \rangle$

Here we present a detailed derivation of various quantities, evolution equations in the new variables, for the linearized dynamics of both the Kuramoto and XY models. To analyze the dynamics (2), as mentioned in the main text, we work in the eigenbasis of the asymmetric Laplacian \mathcal{L} . If $|v_m^R\rangle$ and $\langle v_m^L|$ be the right and left eigenvectors respectively corresponding to an eigenvalue λ_m , we can represent a state, given by the phases of the oscillators, $|\theta\rangle = (\theta_1, \theta_2, \dots, \theta_L)^\top$ in an eigenbasis as follows:

$$|\theta\rangle = \sum_{m=1}^N \langle v_m^L | \theta \rangle |v_m^R\rangle = \sum_{m=1}^N \theta_{\lambda_m}^R |v_m^R\rangle, \quad (\text{A1})$$

$$\langle \theta | = \sum_{m=1}^N \langle \theta | v_m^R \rangle \langle v_m^L | = \sum_{m=1}^N \theta_{\lambda_m}^L \langle v_m^L |. \quad (\text{A2})$$

Similarly, a given realization of the natural frequencies and noise can also be represented by

$$|\omega\rangle = \sum_{m=1}^N \omega_{\lambda_m}^R |v_m^R\rangle, \quad |\eta\rangle = \sum_{m=1}^N \eta_{\lambda_m}^R |v_m^R\rangle, \quad (\text{A3})$$

$$\langle \omega | = \sum_{m=1}^N \omega_{\lambda_m}^L \langle v_m^L |, \quad \langle \eta | = \sum_{m=1}^N \eta_{\lambda_m}^L \langle v_m^L |. \quad (\text{A4})$$

1. Derivation of $\langle \theta_\lambda^L(t) \theta_\lambda^R(t) \rangle$ for the Kuramoto model

We obtain from the linearized Kuramoto dynamics Eq. (2), when projected along the eigenbasis,

$$\begin{aligned} \frac{d\theta_{\lambda_m}^R}{dt} &= -K\lambda_m\theta_{\lambda_m}^R + \omega_{\lambda_m}^R, \\ \frac{d\theta_{\lambda_m}^L}{dt} &= -K\lambda_m\theta_{\lambda_m}^L + \omega_{\lambda_m}^L, \quad m = 1, 2, 3, \dots, N. \end{aligned} \quad (\text{A5})$$

whereas the frequency $\omega_{\lambda_m}^{L,R}$ satisfies

$$\begin{aligned} \langle \omega_{\lambda_m}^{L,R} \rangle &= 0, \\ \langle \omega_{\lambda_m}^L \omega_{\lambda_{m'}}^R \rangle &= \delta_{\lambda_m, \lambda_{m'}}. \end{aligned} \quad (\text{A6})$$

Note that the frequencies $\omega_{\lambda_m}^{L,R}$ for a given λ_m are δ -correlated. The dynamics gets decoupled in the eigen basis and we obtain N independent first order stochastic differential equations. From now on, we use $\omega_\lambda^{L,R}$ instead of $\omega_{\lambda_m}^{L,R}$ for notational convenience. Solution to Eq. (A5) is given by, for $\lambda > 0$,

$$\theta_\lambda^{L/R}(t) = \theta_\lambda^{L/R}(0) e^{-K\lambda t} + \frac{\omega_\lambda^{L/R}}{K\lambda} (1 - e^{-K\lambda t}). \quad (\text{A7})$$

Thus we have

$$\begin{aligned} \langle \theta_\lambda^L(t) \theta_\lambda^R(t) \rangle &= \theta_\lambda^L(0) \theta_\lambda^R(0) e^{-2K\lambda t} \\ &+ \frac{1}{K^2 \lambda^2} (1 - e^{-K\lambda t})^2 \langle \omega_\lambda^L \omega_\lambda^R \rangle, \end{aligned} \quad (\text{A8})$$

$$= \theta_\lambda^L(0) \theta_\lambda^R(0) e^{-2K\lambda t} + \frac{1}{K^2 \lambda^2} (1 - e^{-K\lambda t})^2. \quad (\text{A9})$$

At long times ($t \rightarrow \infty$), it reduces to

$$\langle \theta_\lambda^L(t) \theta_\lambda^R(t) \rangle = \frac{1}{K^2 \lambda^2}. \quad (\text{A10})$$

Equation (A10) is provided in the main text. Note that this result is already provided in Ref. [21]. However, we derive here to make our manuscript self-contained and we generalize this to the case of Gaussian white noise in the next section.

2. Derivation of $\langle \theta_\lambda^L(t) \theta_\lambda^R(t) \rangle$ for the XY model

The governing dynamics (40), once projected along the eigenbasis, yields

$$\begin{aligned} \frac{d\theta_{\lambda_m}^R}{dt} &= -K\lambda_m \theta_{\lambda_m}^R + \eta_{\lambda_m}^R, \\ \frac{d\theta_{\lambda_m}^L}{dt} &= -K\lambda_m \theta_{\lambda_m}^L + \eta_{\lambda_m}^L, \quad m = 1, 2, 3, \dots, N. \end{aligned} \quad (\text{A11})$$

whereas, the noise $\eta_{\lambda_m}^{L,R}(t)$ can easily be shown to follow

$$\begin{aligned} \langle \eta_{\lambda_m}^{L,R}(t) \rangle &= 0, \\ \langle \eta_{\lambda_m}^L(t) \eta_{\lambda_{m'}}^R(t') \rangle &= 2T \delta_{\lambda_m, \lambda_{m'}} \delta(t - t'). \end{aligned} \quad (\text{A12})$$

Here, as well, the noise $\eta_{\lambda_m}^{L,R}(t)$ for a given λ_m are δ -correlated, and the dynamics get decoupled in the eigen basis. Using the notation $\eta_\lambda^{L,R}$ instead of $\eta_{\lambda_m}^{L,R}$, Eq. (A11) yields a formal solution for $\lambda > 0$

$$\theta_\lambda^{L/R}(t) = \theta_\lambda^{L/R}(0) e^{-K\lambda t} + e^{-K\lambda t} \int_0^t dt' \eta_\lambda^{L/R}(t') e^{K\lambda t'} \quad (\text{A13})$$

Note that Eq. (A13) implies for ensemble-averaged

$$\langle \theta_\lambda^{L/R}(t) \rangle = \theta_\lambda^{L/R}(0) e^{-K\lambda t}, \quad (\text{A14})$$

which vanishes as $t \rightarrow \infty$.

One obtains for the quantity

$$\begin{aligned} \langle \theta_\lambda^L(t) \theta_\lambda^R(t) \rangle &= \theta_\lambda^L(0) \theta_\lambda^R(0) e^{-2K\lambda t} \\ &+ e^{-2K\lambda t} \int_0^t dt' \int_0^t dt'' \langle \eta_\lambda^L(t') \eta_\lambda^R(t'') \rangle e^{K\lambda(t'+t'')}, \\ &= \theta_\lambda^L(0) \theta_\lambda^R(0) e^{-2K\lambda t} + 2T e^{-2K\lambda t} \int_0^t dt' e^{2K\lambda t'}, \\ &= \theta_\lambda^L(0) \theta_\lambda^R(0) e^{-2K\lambda t} + \frac{T}{K\lambda} (1 - e^{-2K\lambda t}), \end{aligned} \quad (\text{A15})$$

which yields in the long time limit ($t \rightarrow \infty$)

$$\langle \theta_\lambda^L(t) \theta_\lambda^R(t) \rangle = \frac{T}{K\lambda}. \quad (\text{A16})$$

Equation (A16) is provided in the main text.

-
- [1] S. Boccaletti, V. Latora, Y. Moreno, M. Chavez, and D.-U. Hwang, *Complex networks: Structure and dynamics*, *Physics Reports* **424**, 175 (2006).
- [2] M. E. J. Newman, *Networks* (Oxford University Press, 2010).
- [3] A. Apolloni, C. Poletto, J. J. Ramasco, P. Jensen, and V. Colizza, *Metapopulation epidemic models with heterogeneous mixing and travel behaviour*, *Theoretical Biology and Medical Modelling* **11**, 1 (2014).
- [4] E. Bullmore and O. Sporns, *Complex brain networks: graph theoretical analysis of structural and functional systems*, *Nature Reviews Neuroscience* **10**, 186 (2009).
- [5] G. Petri, P. Expert, H. J. Jensen, and J. W. Polak, *Entangled communities and spatial synchronization lead to criticality in urban traffic*, *Scientific Reports* **3**, 1798 (2013).
- [6] S. N. Dorogovtsev, A. V. Goltsev, and J. F. Mendes, *Critical phenomena in complex networks*, *Reviews of Modern Physics* **80**, 1275 (2008).
- [7] P. Van Mieghem, *Graph Spectra for Complex Networks* (Cambridge University Press, 2023).
- [8] V. Latora, V. Nicosia, and G. Russo, *Complex Networks: Principles, Methods and Applications* (Cambridge University Press, 2017).
- [9] D. Dhar, *Lattices of effectively nonintegral dimensionality*, *Journal of Mathematical Physics* **18**, 577 (1977).
- [10] R. Burioni and D. Cassi, *Universal properties of spectral dimension*, *Physical review letters* **76**, 1091 (1996).
- [11] A. P. Millán, G. Gori, F. Battiston, T. Enss, and N. Defenu, *Complex networks with tuneable spectral dimension as a universality playground*, *Physical Review Research* **3**, 023015 (2021).
- [12] Y. Kuramoto, *Chemical Oscillations, Waves and Turbulence* (Springer, 1984).
- [13] S. H. Strogatz, *From Kuramoto to Crawford: exploring the onset of synchronization in populations of coupled oscillators*, *Physica D: Nonlinear Phenomena* **143**, 1 (2000).
- [14] A. Pikovsky, J. Kurths, M. Rosenblum, and J. Kurths, *Synchronization: A Universal Concept in Nonlinear Sciences*, Vol. 12 (Cambridge University Press, 2003).
- [15] J. A. Acebrón, L. L. Bonilla, C. J. P. Vicente, F. Ri-

- tort, and R. Spigler, The kuramoto model: A simple paradigm for synchronization phenomena, *Reviews of Modern Physics* **77**, 137 (2005).
- [16] D. Cassi, Phase transitions and random walks on graphs: A generalization of the mermin-wagner theorem to disordered lattices, fractals, and other discrete structures, *Physical Review Letters* **68**, 3631 (1992).
- [17] D. Cassi, Local vs average behavior on inhomogeneous structures: Recurrence on the average and a further extension of Mermin-Wagner theorem on graphs, *Physical Review Letters* **76**, 2941 (1996).
- [18] M. Sarkar, Noise-induced synchronization in the Kuramoto model on finite 2D lattice, arXiv preprint arXiv:2004.00294 (2020).
- [19] M. Sarkar, Synchronization transition in the two-dimensional Kuramoto model with dichotomous noise, *Chaos: An Interdisciplinary Journal of Nonlinear Science* **31** (2021).
- [20] R. Burioni, D. Cassi, and A. Vezzani, Inverse mermin-wagner theorem for classical spin models on graphs, *Phys. Rev. E* **60**, 1500 (1999).
- [21] A. P. Millán, J. J. Torres, and G. Bianconi, Synchronization in network geometries with finite spectral dimension, *Physical Review E* **99**, 022307 (2019).
- [22] G. Ódor and S. Deng, Synchronization transition of the second-order kuramoto model on lattices, *Entropy* **25**, 164 (2023).
- [23] S. Gupta and S. Ruffo, The world of long-range interactions: A bird's eye view, *International Journal of Modern Physics A* **32**, 1741018 (2017).
- [24] P. Grassberger, SIR epidemics with long-range infection in one dimension, *Journal of Statistical Mechanics: Theory and Experiment* **2013**, P04004 (2013).
- [25] G. Gori, M. Michelangeli, N. Defenu, and A. Trombettoni, One-dimensional long-range percolation: A numerical study, *Physical Review E* **96**, 012108 (2017).
- [26] M. Ibáñez Berganza and L. Leuzzi, Critical behavior of the XY model in complex topologies, *Physical Review B* **88**, 144104 (2013).
- [27] F. Cescatti, M. Ibáñez-Berganza, A. Vezzani, and R. Burioni, Analysis of the low-temperature phase in the two-dimensional long-range diluted XY model, *Physical Review B* **100**, 054203 (2019).
- [28] P. Grassberger, Two-dimensional SIR epidemics with long range infection, *Journal of Statistical Physics* **153**, 289 (2013).
- [29] G. Bighin, T. Enss, and N. Defenu, Universal scaling in fractional dimension, arXiv:2211.13302 (2022).
- [30] *STOC '00: Proceedings of the Thirty-Second Annual ACM Symposium on Theory of Computing* (Association for Computing Machinery, New York, NY, USA, 2000).
- [31] D. J. Watts and S. H. Strogatz, Collective dynamics of 'small-world' networks, *Nature* **393**, 440 (1998).
- [32] S. Carmi, S. Carter, J. Sun, and D. Ben-Avraham, Asymptotic behavior of the Kleinberg model, *Physical Review Letters* **102**, 238702 (2009).
- [33] C. C. Cartozo and P. De Los Rios, Extended navigability of small world networks: exact results and new insights, *Physical Review Letters* **102**, 238703 (2009).
- [34] G. Li, S. D. S. Reis, A. A. Moreira, S. Havlin, H. E. Stanley, and J. S. Andrade Jr, Towards design principles for optimal transport networks, *Physical Review Letters* **104**, 018701 (2010).
- [35] S. Gupta, A. Campa, and S. Ruffo, *Statistical Physics of Synchronization* (Springer, 2018).
- [36] R. Burioni and D. Cassi, Geometrical universality in vibrational dynamics, *Modern Physics Letters B* **11**, 1095 (1997).
- [37] R. Livi and P. Politi, *Nonequilibrium Statistical Physics A Modern Perspective* (Cambridge University Press, 2017).
- [38] J. M. Kosterlitz and D. J. Thouless, Ordering, metastability and phase transitions in two-dimensional systems, *Journal of Physics C: Solid State Physics* **6**, 1181 (1973).
- [39] J. M. Kosterlitz, The critical properties of the two-dimensional XY model, *Journal of Physics C: Solid State Physics* **7**, 1046 (1974).
- [40] N. D. Mermin and H. Wagner, Absence of ferromagnetism or antiferromagnetism in one-or two-dimensional isotropic heisenberg models, *Physical Review Letters* **17**, 1133 (1966).
- [41] G. Giachetti, N. Defenu, S. Ruffo, and A. Trombettoni, Berezinskii-Kosterlitz-Thouless phase transitions with long-range couplings, *Physical Review Letters* **127**, 156801 (2021).
- [42] J. M. Kosterlitz, Phase transitions in long-range ferromagnetic chains, *Physical Review Letters* **37**, 1577 (1976).
- [43] R. Brown and E. Šimánek, Monte Carlo simulation of the $1/n^2$ plane rotator chain, *Physical Review B* **38**, 9264 (1988).
- [44] C. Godsil and G. F. Royle, *Algebraic graph theory*, Vol. 207 (Springer Science & Business Media, 2001).
- [45] H. Hong, H. Park, and M. Choi, Collective synchronization in spatially extended systems of coupled oscillators with random frequencies, *Physical Review E* **72**, 036217 (2005).
- [46] N. G. Van Kampen, *Stochastic processes in physics and chemistry*, Vol. 1 (Elsevier, 1992).
- [47] D. Chowdhury and M. C. Cross, Synchronization of oscillators with long-range power law interactions, *Physical Review E* **82**, 016205 (2010).
- [48] K. Binder, Finite size scaling analysis of Ising model block distribution functions, *Zeitschrift für Physik B* **43**, 119 (1981).
- [49] D. P. Landau and K. Binder, *A Guide to Monte Carlo Simulations in Statistical Physics* (Cambridge University Press, 2009).
- [50] G. Wysin, A. Pereira, I. Marques, S. Leonel, and P. Coura, Extinction of the Berezinskii-Kosterlitz-Thouless phase transition by nonmagnetic disorder in planar symmetry spin models, *Physical Review B* **72**, 094418 (2005).